сообщения
объединенного
института
ядерных
исследований
дубна

E1-90-185

P. Kozma

SYSTEMATICS OF TARGET RECOIL PROPERTIES OF INTERMEDIATE FRAGMENTS PRODUCED IN THE INTERACTION OF 3.65 AGeV ^{12}C-IONS AND PROTONS WITH COMPLEX NUCLEI

1990

1. Introduction

One of the most interesting features of the reactions induced by relativistic projectiles is a large yield of intermediate / $A \lesssim 30$ / fragments. The possibility that the emission of these fragments may involve the formation of nuclear matter in a state of abnormally high temperature or density renders the studies of this type one of continuing interest.

The emission of intermediate fragments in reactions of relativistic projectiles with complex nuclei can be studied particularly by measurements of their recoil properties. The thick-target, thick-catcher technique, in which both target and catchers are thick compared to the range of the fragments of interest, has been used extensively [1-6]. Recoiling nuclei are collected in 2π geometry and the fraction which recoils out of the target in the forward and backward directions with respect to the beam is measured. The experimental results are expressed as the ratios of forward-to-backward emission, F/B, and the mean ranges in the target material, 2W(F+B): F and B are the fractional numbers of fragment recoiling into the forward and backward catcher, respectively, W is the target thickness in mg/cm^2.

By using a well-known activation technique we have measured mean ranges and forward-to-backward ratios of the ^{24}Na and ^{28}Mg radionuclides produced in the interaction of 3.65 AGeV ^{12}C-ions and 3.65 GeV protons with complex nuclei: Mn, Co, Cu, Y, Nb, Ag, Tb, Ta, Au, Pb, Th and U. The experiments were performed in conjunction with the cross sections determination previously reported in refs. [7-14]. In the present work the results of recoil properties are summarized and the systematics of kinematic properties and their dependence on target mass are examined. The results are discussed within the theoretical framework of the vector velocity model [15]. A preliminary analysis of the results has been also given in refs. [16-18].

2. Experimental

The experimental procedure is described in detail in [18]. Briefly, the experiments involved irradiations of appropriate target foils by 3.65 GeV protons and 3.65 AGeV ^{12}C-ions at the external beam of the Dubna synchrophasotron. The targets ranging in thickness from 20 mg/cm^2 /Th/ to 62 mg/cm^2 /Pb/ were placed between 17.5 mg/cm^2 thick Mylar catcher foils. After irradiation the target stacks were disassembled and appropriate forward, F, and backward, B, catcher foils were assayed with Ge/Li/ gamma-ray spectrometers. The gamma-ray spectra were analyzed with the codes SAMPO[19] and GSAP[20]. The activities of ^{24}Na and ^{28}Mg were determined in the various catchers from counting rates of the most intense gamma-rays.

3. Results and analysis

The mean ranges in the targets, 2W(F+B), and the ratios of forward-to-backward emission, F/B, are summarized in Table 1 and also displayed in Figs.1 and 2, respectively, as plots of the F/B and 2W(F+B) versus target A_T for both fragments in question.

Table 1 Recoil properties of ^{24}Na and ^{28}Mg fragments emitted in the reactions of 3.65 AGeV projectiles with the listed targets

Reaction	^{24}Na fragment		^{28}Mg fragment	
	F/B	2W(F+B) [mg/cm^2]	F/B	2W(F+B) [mg/cm^2]
p + ^{55}Mn	3.15 ± 0.20	2.42 ± 0.24	3.13 ± 0.21	2.40 ± 0.24
p + ^{59}Co	2.89 ± 0.20	2.74 ± 0.25	2.89 ± 0.22	2.75 ± 0.25
p + ^{64}Cu	2.63 ± 0.18	2.79 ± 0.22	2.57 ± 0.20	3.02 ± 0.25
p + ^{89}Y	2.21 ± 0.15	4.00 ± 0.42	2.30 ± 0.18	3.69 ± 0.51
p + ^{93}Nb	2.25 ± 0.15	3.80 ± 0.39	2.26 ± 0.17	3.58 ± 0.42
p + ^{108}Ag	2.19 ± 0.17	4.35 ± 0.37	2.14 ± 0.18	4.77 ± 0.42
p + ^{159}Tb	2.04 ± 0.12	7.42 ± 1.28	1.95 ± 0.15	8.30 ± 1.30
p + ^{181}Ta	2.01 ± 0.11	10.56 ± 1.45	1.86 ± 0.12	12.48 ± 1.50
p + ^{197}Au	1.76 ± 0.15	11.93 ± 1.74	1.66 ± 0.15	13.90 ± 2.02
p + $^{207.2}$Pb	1.83 ± 0.12	10.89 ± 1.64	1.85 ± 0.18	12.47 ± 1.88
^{12}C + ^{55}Mn	3.93 ± 0.35	3.15 ± 0.32	3.74 ± 0.34	2.90 ± 0.27
^{12}C + ^{59}Co	4.05 ± 0.37	3.33 ± 0.35	3.69 ± 0.35	3.03 ± 0.33
^{12}C + ^{64}Cu	3.26 ± 0.28	3.95 ± 0.38	3.08 ± 0.30	2.94 ± 0.31
^{12}C + ^{108}Ag	2.67 ± 0.23	5.18 ± 0.54	2.44 ± 0.26	5.60 ± 0.58
^{12}C + ^{181}Ta	2.32 ± 0.14	12.88 ± 1.67	2.20 ± 0.14	14.23 ± 1.73
^{12}C + ^{197}Au	2.12 ± 0.21	14.63 ± 1.80	1.81 ± 0.21	15.25 ± 1.89
^{12}C + $^{207.2}$Pb	1.96 ± 0.20	14.09 ± 1.34	1.80 ± 0.23	15.32 ± 1.72
^{12}C + ^{232}Th	2.05 ± 0.26	15.05 ± 2.18	1.90 ± 0.25	15.44 ± 2.25
^{12}C + ^{238}U	2.00 ± 0.25	15.07 ± 2.11	1.85 ± 0.25	16.30 ± 2.40

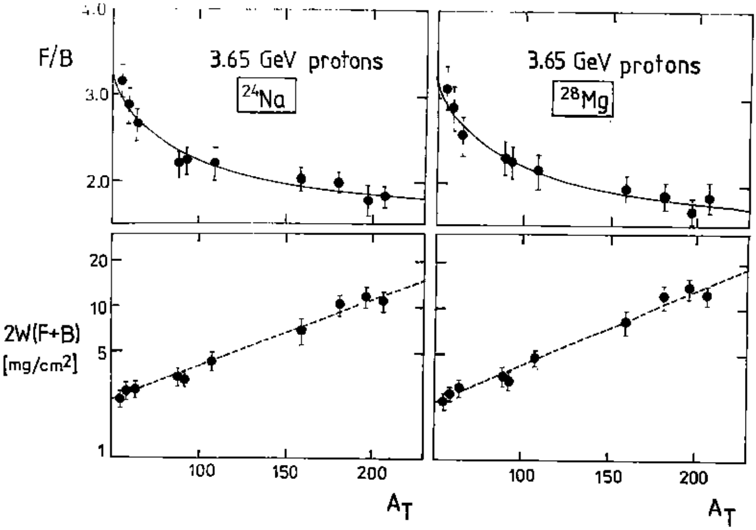

Fig. 1. Forward-to-backward ratios and mean ranges of ^{24}Na and ^{28}Mg fragments emitted in the interaction of 3.65 GeV protons with targets of mass A_T. The curves show the trends in the data.

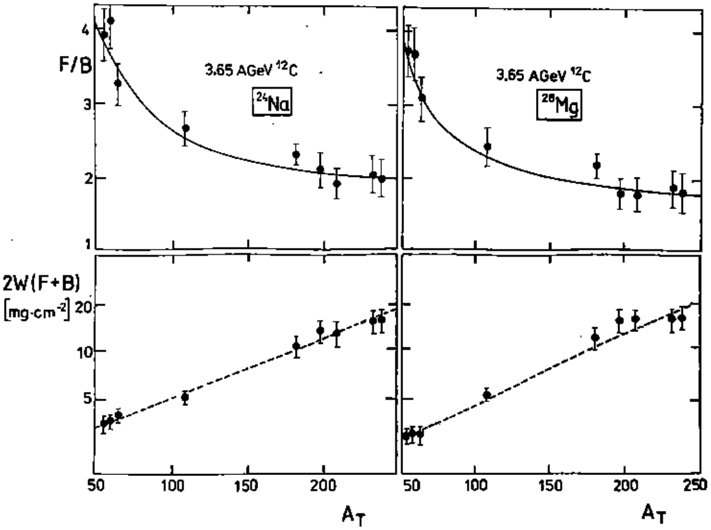

Fig. 2. Forward-to-backward ratios and mean ranges of ^{24}Na and ^{28}Mg fragments emitted in the interaction of 3.65 AGeV ^{12}C-ions with targets of mass A_T. The curves show the trends in the data.

The analysis of the recoil data in terms of the two-step velocity vector model [15] is based on the next assumptions: the observed velocity of a recoil product $\vec{v}_r$ can be divided into two components $\vec{v}$ and $\vec{V}$ corresponding to the cascade and break-up stage of the interaction . In the first step of the interaction the incident projectile interacts with the target nucleus and imparts a velocity $v_{\parallel}$ along the beam direction to the resulting residual nucleus. The break-up of this remnant leads to isotropic emission in the moving system of a fragment with a velocity V. By using the notation

$$\eta_{\parallel} = v_{\parallel}/V \ , \qquad /1/$$

/the perpendicular component of the cascade velocity $v_{\perp}$ is assumed to be zero/, and

$$R_o = kv^N \ , \qquad /2/$$

Table 2 Summary of ^{24}Na results

Reaction	$\eta_{\parallel}$	R_o [mg/cm^2]	T [MeV]	$v_{\parallel}$ [MeV/A]$^{1/2}$	⟨P⟩ [MeV.A]$^{1/2}$
p + ^{55}Mn	0.241	2.268	10.0±0.5	0.221±0.026	12.1±1.4
p + ^{59}Co	0.224	2.590	12.1±0.6	0.227±0.027	13.3±1.7
p + ^{64}Cu	0.204	2.662	12.2±0.6	0.207±0.022	13.2±1.4
p + ^{89}Y	0.168	3.874	14.5±0.7	0.184±0.020	16.4±1.8
p + ^{93}Nb	0.172	3.674	14.3±0.7	0.187±0.021	17.4±2.0
p + ^{108}Ag	0.166	4.216	15.1±0.8	0.187±0.021	20.2±2.3
p + ^{159}Tb	0.151	7.229	25.0±1.3	0.218±0.025	34.7±4.0
p + ^{181}Ta	0.148	10.298	36.5±1.8	0.258±0.038	46.7±6.9
p + ^{197}Au	0.120	11.735	45.0±2.2	0.234±0.038	46.2±7.5
p + $^{207.2}$Pb	0.128	10.687	40.0±2.1	0.235±0.039	48.8±8.0
^{12}C + ^{55}Mn	0.286	2.878	12.0±1.0	0.288±0.039	15.8±2.2
^{12}C + ^{59}Co	0.292	3.031	12.5±1.1	0.300±0.042	17.7±2.5
^{12}C + ^{64}Cu	0.248	3.687	14.0±1.3	0.269±0.035	17.2±2.2
^{12}C + ^{108}Ag	0.207	4.935	17.2±1.8	0.249±0.033	26.9±3.6
^{12}C + ^{181}Ta	0.178	12.424	44.5±6.0	0.342±0.051	61.9±9.2
^{12}C + ^{197}Au	0.159	14.213	54.5±6.5	0.305±0.048	60.0±9.5
^{12}C + $^{207.2}$Pb	0.143	13.766	52.0±5.0	0.298±0.042	61.7±8.6
^{12}C + ^{232}Th	0.152	14.658	61.5±9.0	0.344±0.065	79.8±15
^{12}C + ^{238}U	0.147	14.703	62±8	0.344±0.054	79.5±13

Table 3 Summary of ^{28}Mg results

Reaction	η_w	R_0 $[mg/cm^2]$	T $[MeV]$	v_w $[MeV/A]^{1/2}$	$\langle P \rangle$ $[MeV.A]^{1/2}$
$p + {}^{55}Mn$	0.241	2.268	10.0 ± 0.6	0.204 ± 0.025	11.2 ± 1.4
$p + {}^{59}Co$	0.225	2.599	12.0 ± 0.6	0.208 ± 0.025	12.3 ± 1.5
$p + {}^{64}Cu$	0.200	2.886	12.7 ± 0.7	0.190 ± 0.024	12.2 ± 1.6
$p + {}^{89}Y$	0.177	3.520	13.3 ± 0.8	0.173 ± 0.018	15.4 ± 1.7
$p + {}^{93}Nb$	0.173	3.425	13.2 ± 0.8	0.168 ± 0.015	15.6 ± 1.8
$p + {}^{108}Ag$	0.162	4.630	15.6 ± 0.9	0.171 ± 0.021	18.5 ± 2.2
$p + {}^{159}Tb$	0.142	8.047	28.0 ± 1.5	0.200 ± 0.023	32.0 ± 3.7
$p + {}^{181}Ta$	0.132	12.177	46.5 ± 2.8	0.241 ± 0.035	43.5 ± 6.3
$p + {}^{197}Au$	0.108	13.714	52.5 ± 2.9	0.209 ± 0.036	41.2 ± 7.2
$p + {}^{207.2}Pb$	0.131	12.226	48 ± 3	0.243 ± 0.044	50.3 ± 9.1
${}^{12}C + {}^{55}Mn$	0.278	2.663	11.8 ± 1.0	0.255 ± 0.033	14.0 ± 1.8
${}^{12}C + {}^{59}Co$	0.286	2.769	12.0 ± 1.0	0.265 ± 0.038	15.6 ± 2.3
${}^{12}C + {}^{64}Cu$	0.237	2.760	12.0 ± 1.2	0.219 ± 0.031	14.0 ± 2.0
${}^{12}C + {}^{108}Ag$	0.189	5.377	18.5 ± 1.9	0.217 ± 0.032	23.5 ± 3.5
${}^{12}C + {}^{181}Ta$	0.167	13.786	46.5 ± 4.5	0.305 ± 0.039	60.7 ± 7.1
${}^{12}C + {}^{197}Au$	0.127	14.082	62.5 ± 5.8	0.268 ± 0.046	52.9 ± 9.0
${}^{12}C + {}^{207.2}Pb$	0.126	15.065	63.0 ± 6.2	0.267 ± 0.045	55.4 ± 9.4
${}^{12}C + {}^{232}Th$	0.136	15.116	63.5 ± 6.5	0.290 ± 0.038	67.3 ± 8.8
${}^{12}C + {}^{238}U$	0.130	15.985	68.5 ± 8.0	0.287 ± 0.040	68.3 ± 9.5

Table 4 Mean ranges as a function of mass target

Reaction	Range
$A_T(p,X)^{24}Na$	$R_0 = 1.373 \exp(0.0105 A_T)$
$A_T(p,X)^{28}Mg$	$R_0 = 1.268 \exp(0.0116 A_T)$
$A_T({}^{12}C,X)^{24}Na$	$R_0 = 1.859 \exp(0.0093 A_T)$
$A_T({}^{12}C,X)^{28}Mg$	$R_0 = 1.555 \exp(0.0104 A_T)$

/R_o is the mean range in the target material, corresponding to the recoil speed V, k and N being constants/, the following relations were derived:

$$2W(F+B) = R_o\left[1 + \frac{1}{4}\eta_{\parallel}^2(N+1)^2\right] \qquad /3/$$

and

$$F/B = \frac{1 + 2/3\,\eta_{\parallel}(N+2) + 1/4[\eta_{\parallel}(N+1)]^2}{1 - 2/3\,\eta_{\parallel}(N+2) + 1/4[\eta_{\parallel}(N+1)]^2} \;. \qquad /4/$$

The parameters of interest are the fragment kinetic energy

$$T = \frac{1}{2}AV^2 \;, \qquad /5/$$

the velocity imparted to the progenitor of the fragment

$$v_{\parallel} = \eta_{\parallel}\sqrt{\frac{2T}{A}} \;, \qquad /6/$$

and the average momentum imparted to the struck nuclei in the beam direction

$$\langle P\rangle = v_{\parallel} x A_T \;. \qquad /7/$$

These kinematic parameters were obtained from experimental data using Eqs./1/ and /2/ for N=1, the range-energy tables of Northcliffe and Schilling [21] and relationships derived by Winsberg [22] from experimental stopping powers. The results for ^{24}Na and ^{28}Mg fragments are summarized in Table 2 and 3, respectively. The appropriate range-mass target relationships in the form

$$R_o = a\,\exp(bA_T) \;, \qquad /8/$$

obtained by means of the LSQ fitting procedure are displayed in Table 4.

4. Discussion

The dependence of the fragment kinetic energy on the fractional mass loss, $\Delta A/A_T$, ΔA being the mass difference between target and product, is displayed in Fig.3. Cumming and Bächmann [23] and Winsberg [24] have systemized the kinetic energies of spallation products on the basis of assumptions related to the random nature of individual steps. They have shown that kinetic energies should increase linearly with $\Delta A/A_T$. As can be seen from Fig.3, the expected linear dependence in both interactions is valid up to $\Delta A/A_T \approx 0.8$. Next, a sharp increase of kinetic energies of both fragments emitted from lighter target nuclei in both interactions is clearly evident. This effect may be caused by a change in reaction mechanism: a clustering of nucleons into intermediate mass fragments in the vicinity of a liquid-gas transition critical point [25].

In Fig.4 we display the dependences of velocity of remnants $\beta_{\parallel}=v_{\parallel}/c$ for proton and ^{12}C-ion induced reactions on fractional mass loss. Taking into account that appropriate forward momenta of remnants $\beta_{\parallel}A_T$ are proportional to the excitation energies and, consequently, to the

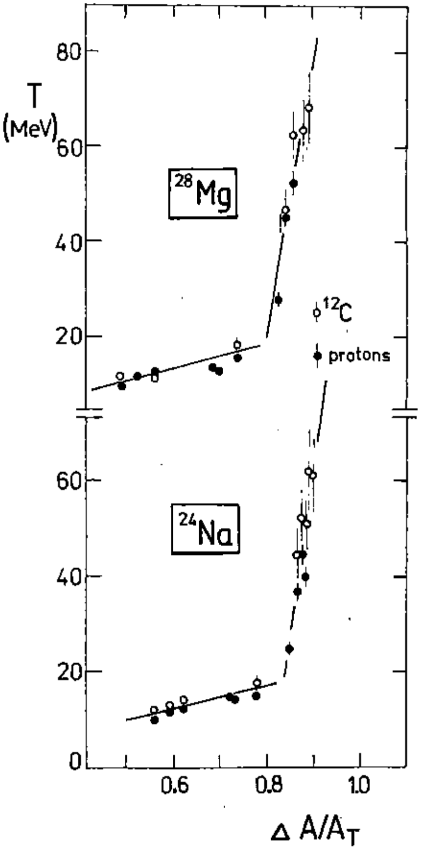

Fig.3. Dependence of the mean fragment kinetic energy T on fractional mass loss $\Delta A/A_T$ in reactions induced by 3.65 AGeV ^{12}C-ions and 3.65 GeV protons. The straight lines show the general behavior of the experimental points.

mass loss, $\beta_{\parallel}$ values should increase with $\Delta A/A_T$. However, no increase from Fig.4 can be seen: the values of $\beta_{\parallel}$ vary slowly with fractional mass loss without any discernible systematics trends. Nevertheless, the similarity of both $\beta_{\parallel}$ values for both projectiles do not contradict the factorization hypothesis [26].

In Fig.5 we compare the values of $\beta_{\parallel}$ deduced from the present recoil data for 3.65 AGeV ^{12}C-ions with those obtained previously at 1.54 AGeV ^{12}C projectiles [5]. Finally, in Fig.6 and 7 we show the va-

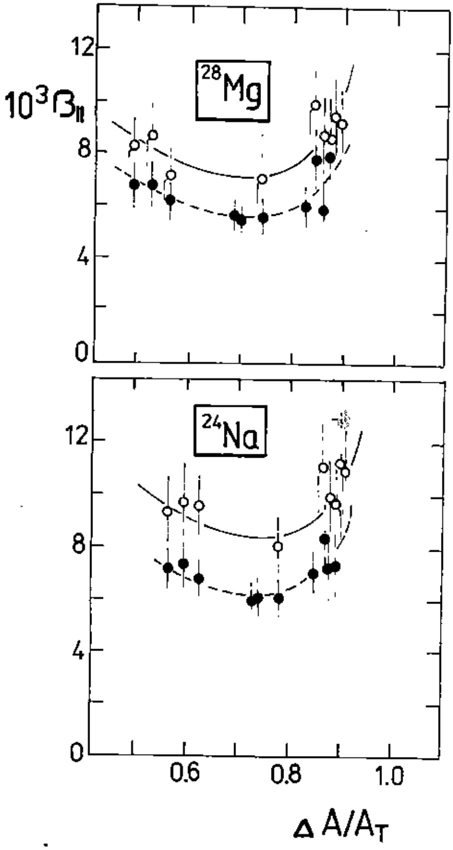

Fig.4. Dependence of velocity $\beta_\parallel$ on fractional mass loss $\Delta A/A_T$ in reactions induced by 3.65 AGeV ^{12}C-ions /open points/ and 3.65 GeV protons /full points/. The appropriate curves are drawn to guide the eye.

riation of velocities with incident proton energy for copper, silver and gold target nuclei and both emitted fragment, ^{24}Na and ^{28}Mg, respectively. The curves are drawn to guide the eye. It is seen that except for the point at 3 GeV for ^{197}Au target nuclei general trends of data follow the limiting fragmentation [27].

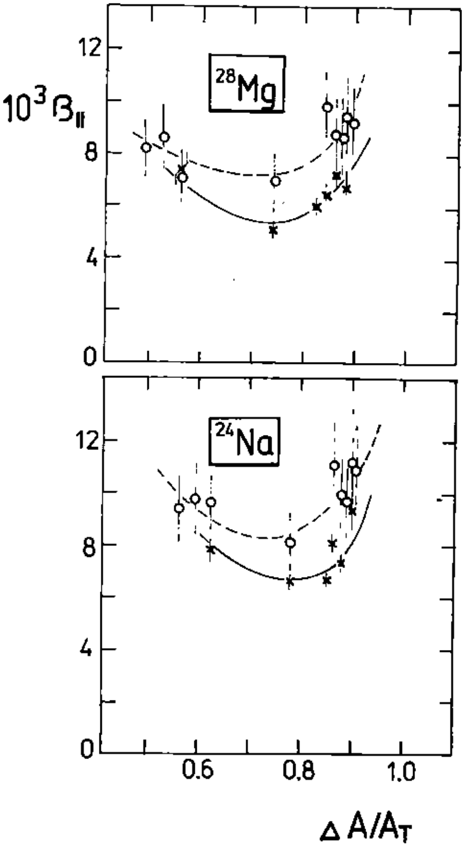

Fig.5. Comparison of $\beta_{\parallel}$ value dependences on $\Delta A/A_T$ in reactions induced by 3.65 AGeV ^{12}C-ions /open points/ with those induced by 1.54 AGeV ^{12}C-ions /cross points/ [5]. The appropriate curves are drawn to guide the eye.

5. Conclusions

The recoil properties of ^{24}Na and ^{28}Mg intermediate fragments produced in the interaction of various target nuclei with 3.65 AGeV ^{12}C ions and 3.65 GeV protons have been systemized by means of the two-

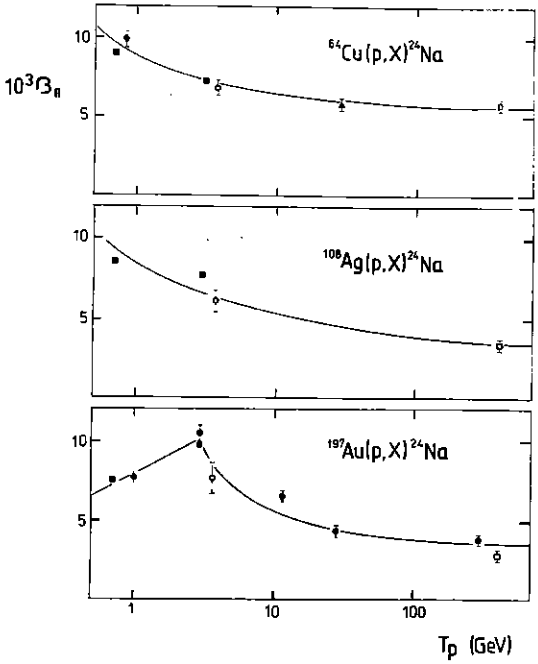

Fig.6. Variation of β_* with incident proton energy for copper, silver and gold target nuclei and emitted fragment of ^{24}Na: o - present results;
● - Kaufmann et al. [3]; ■ - Crespo et al. [1];
▲ - Cumming et al. [4a]; ◆ - Cumming et al. [4b];
□ - Cole and Porile [5]. The curves show the general behavior of the data.

step vector velocity model. Kinematic parameters, such as mean fragment kinetic energies and velocities of appropriate remnants have been deduced and compared for both interactions and other available data, as well. The applicability of kinematic parameters to test the hypotheses of factorization and limiting fragmentation has also been demonstrated.

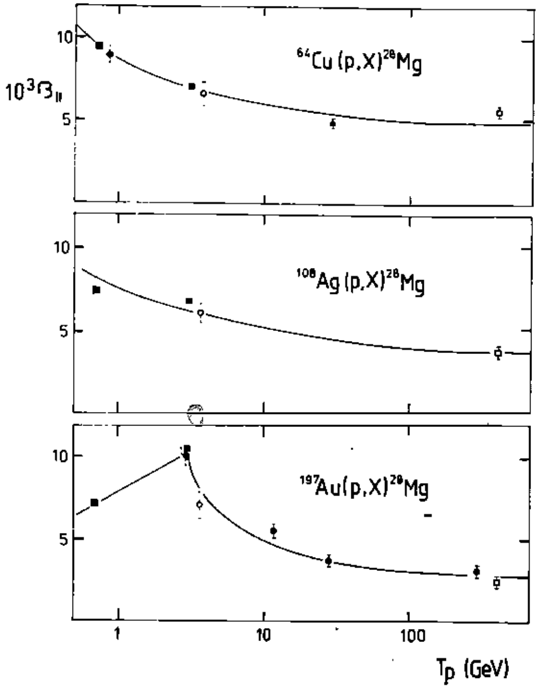

Fig.7. Variation of $\beta_\parallel$ with incident proton energy for copper, silver and gold target nuclei and emitted fragment of ^{28}Mg. The symbols are the same as in Fig.6, the curves show the general behavior of the data.

References

1. V.P.Crespo,J.M.Alexander and E.K.Hyde, Phys.Rev.131,1963,p.1765.
2. V.P.Crespo,J.B.Cumming and J.M.Alexander, Phys.Rev.C2,1970,p.1777.
3. S.B.Kaufman,E.P.Steinberg and M.H.Weisfield, Phys.Rev.C18,1978,p. 1346.
4. J.B.Cumming,P.E.Haustein and H.-C.Hseuh, Phys.Rev.C18,1978,p.1372; Phys.Rev.C24,1981,p.2162.
5. G.D.Cole and N.T.Porile, Phys.Rev.C24,1981,p.2038; Phys.Rev.C25, 1982,p.244.

6. C.F.Wang and N.T.Porile, Nucl.Phys.A468,1987,p.711.
7. P.Kozma,J.Kliman and M.Leonard, Czech.J.Phys.B38,1988,p.973.
8. P.Kozma and J.Kliman, Czech.J.Phys.B38,1988,p.1317.
9. P.Kozma,C.Damdinsuren,D.Chultem and B.Tumendemberel, JINR Report E1-89-252,1989,Dubna.
10. P.Kozma,B.Tumendemberel and D.Chultem, JINR Report E1-88-244,1988, Dubna; and to be published.
11. P.Kozma and C.Damdinsuren, JINR Report E1-88-245,1988,Dubna.
12. C.Damdinsuren,V.I.Ilyushchenko,P.Kozma and D.Chultem, JINR Report E1-89-481,1989,Dubna.
13. P.Kozma,V.I.Ilyushchenko and J.Kliman, JINR Report E1-89-482,1989, Dubna; and to be published.
14. P.Kozma and J.Kliman, J.Phys.G.:Nucl.Part.Phys.16,1990,p.45.
15. N.Sugarman et al., Phys.Rev.143,1966,p.952.
16. P.Kozma,J.Kliman and M.Leonard, Proc.of the 38th Conference on Nuclear Spectroscopy, Baku,1988,p.304.
17. P.Kozma and J.Kliman, Phys.and Appl.15,1988,p.77.
18. P.Kozma, Czech.J.Phys.B40,1990,93.
19. M.J.Koskelo,P.A.Aarnio and J.T.Routti, Nucl.Instr.and Meth. 190, 1981,p.89.
20. V.Hnatowicz,V.I.Ilyushchenko and P.Kozma, Comp.Phys.Comm.,inprint; and JINR Report E10-89-758,1989,Dubna.
21. L.C.Northcliffe and R.F.Schilling, Nucl.Data Tables A7,1970,p.233.
22. L.Winsberg, Nucl.Instr. and Meth.150,1978,p.465.
23. J.B.Cumming and K.Bächmann, Phys.Rev. C6,1972,p.1362.
24. L.Winsberg, Phys.Rev.C22,1980,p.2123.
25. A.S.Hirsch et al., Phys.Rev.C29,1984,p.508.
26. R.P.Feynman, Phys.Rev.Lett.23,1969,p.1415.
27. J.Benecke,T.T.Chou,N.C.Young and E.Yen, Phys.Rev.188,1969,p.2159.

Received by Publishing Department
of March 13, 1990.